Enzymatic Activation Complex Formation Induced by Crowding Stress

Lalita Shahu, Dedunu S. Senarathne, Sandipan Saha, H. Peter Lu*

Bowling Green State University, Department of Chemistry, Center for Photochemical Sciences, Bowling Green, OH 43403 *Corresponding Author: E-mail: hplu@bgsu.edu.

S1: Sample preparation

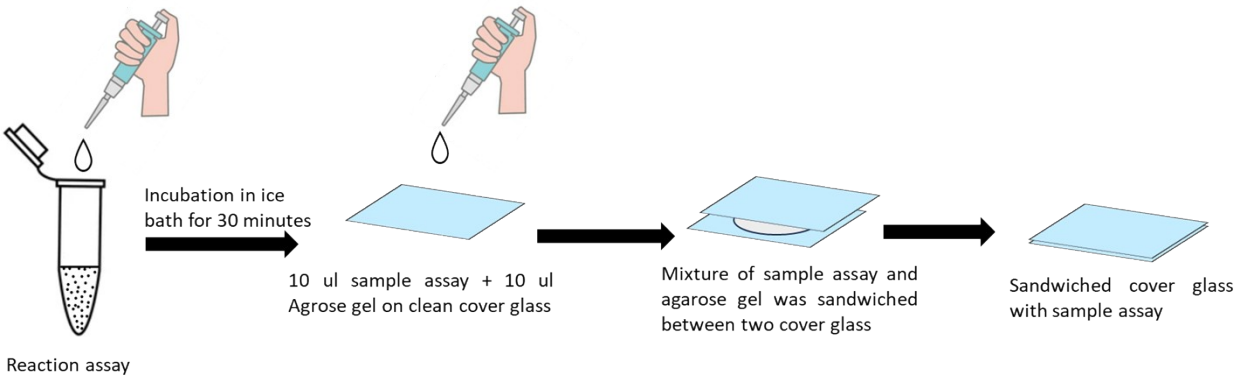

Figure S1: Schematic representation of cover glass preparation with sample assay.

Our Sample assay was prepared in 50 mM HEPES buffer (pH 7.4) with glycerol 10% v/v and 100 mM NaCl. All the necessary components in the sample assay consist of NADPH (100 µM), L-Arginine (100 µM), Tetrahydrobiopterin (H_4B) 10 µM, and eNOS 30 nM, Cy3- Cy5 labelled Calmodulin (CaM); 2 nM, Ficoll 70 of different concentrations in our crowding experiments. Control experiment with no macromolecular crowding consists of 200 µM $CaCl_2$ in place of Ficoll 70. Here sample assay is mixed quickly with the agarose gel at its gelling temperature. Agarose gel at its gelling temperature forms a large number of compartments or chambers ~200-300 nm.[1] The sample assays are confined within these nanoscale chambers. With the 2 nM concentration of Cy3-Cy5 labeled calmodulin (CaM), a single molecule of CaM is likely to be captured within each chamber. This setup allows for the straightforward investigation of binding events between CaM and endothelial nitric oxide synthase (eNOS).

S2: sm FRET Experimental setup, imaging, and FRET efficiency quantification

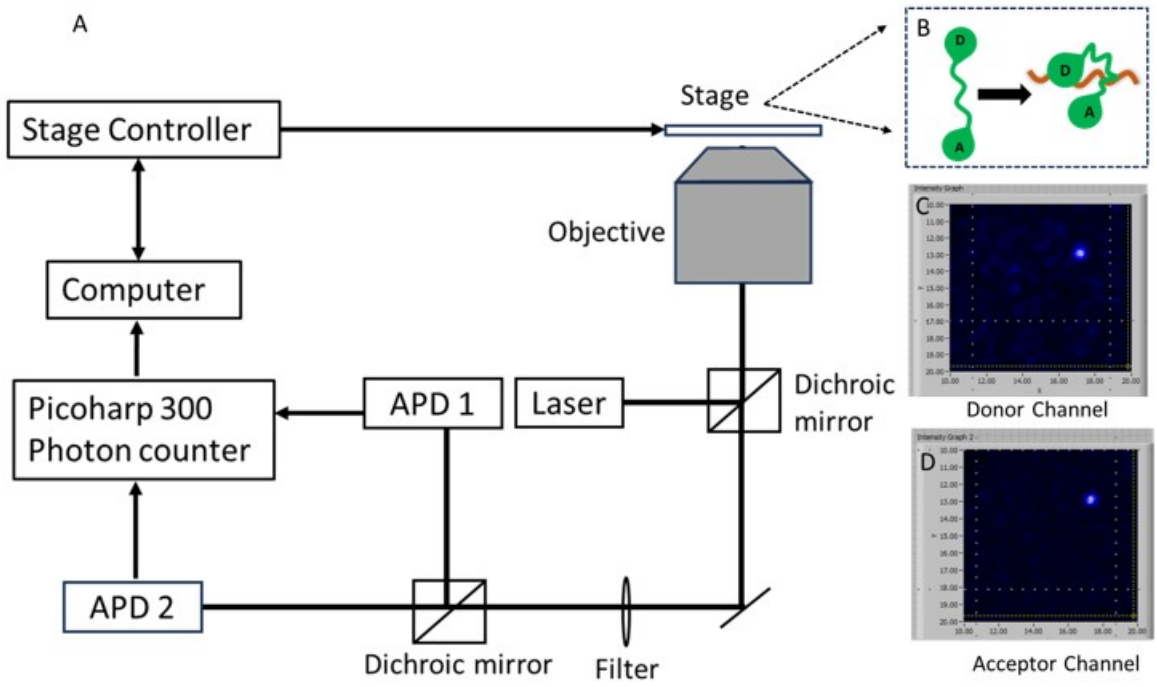

Figure S2: Schematic representation of a single-molecule fluorescent experimental setup. (A) Experimental setup with 532 nm (CW) laser as an excitation source; two-channel photon detector (APD1 and APD2); objective; and dichroic mirror. (B) Schematic representation of calmodulin- NOS interdomain linker interaction in the tens of µm-sized chamber formed in agarose gel. (C and D) single-molecule fluorescence image (10 µm x 10 µm) in donor and acceptor channels.

Our home-built experimental setup primarily consists of an inverted optical microscope (Axiovert-200, Zeiss). The excitation laser (532 nm) beam was reflected by a dichroic beamsplitter (z532rdc, Chroma Technology) and focused by a high-numerical-aperture objective (1.3NA, 100X, Zeiss) on the sample surface at a diffraction-limited spot of about 300 nm in diameter. To obtain photon-counting time trajectories, the emission signal from Cy3 and Cy5 was collected using a dichroic beam splitter (640dcxr) by Si avalanche photodiode single photon counting modules (SPCM-AQR-16, Perkin Elmer Optoelectronics) for detecting the fluorescence. We were able to obtain a fluorescence image scanning 10µm × 10µm by continuously raster-scanning the sample over the laser focus with a piezoelectric scanning stage (Physik Instruments Inc., Germany) at any scanning speed (typically 4 ms/pixel). Typically, we collect fluorescence intensity from Cy3 and Cy5 for 40 seconds with a two-channel Picoharp 300 (PicoQuant). Mirror; Dichroic beam splitter 1: z532rdc (Chroma Technology), reflecting 532 nm excitation laser beam and transmitting fluorescence. Dichroic beam splitter 2: 640dcxr (Chroma Technology), can split the emission signal into two color beams. We use APD for recording the intensity. APD 1 and APD 2: Si avalanche photodiode single photon counting modules (SPCM-AQR-16, Perkin Elmer Optoelectronics) for detecting the single-molecule fluorescence from Cy3 (570 nm) emission and Cy5 (670 nm) emission filter 1: HQ545lp (Chroma Technology), blocking 532 nm excitation laser beam. Figure S2 (B) shows a schematic representation showing the dye-labelled calmodulin in the sandwiched sample on the x−y closed-loop piezo position scanning stage for raster-scan. After scanning in a 10 µm x 10 µm area, we can get the two-dimensional single molecule fluorescence image in both the channels shown as bright spots in Figure S2 (C and D).

In our experiments, the measured FRET efficiencies reflect relative distance changes between donor and acceptor fluorophores. To convert these efficiency values into absolute distances, calibration requires an accurate Förster radius (R_0) and assumptions about the rotational freedom and orientation factor (κ^2) of the fluorophores. Additionally, the presence of flexible linkers and local environment effects can introduce uncertainties in exact distance calculations. Absolute distance determination is challenging hence we have performed internal calibrations using known reference distances and control experiments to relate changes in FRET efficiency to approximate distance changes. These calibrations allow us to interpret relative distance fluctuations that correspond to protein conformational dynamics within ranges typically sensitive to FRET (approximately 2–8 nm).

Some limitations such as dye labeling perturbation and dye photobleaching could be present in this method. However, we have followed our standard protocol in sample preparation to avoid such limitations.

Single-molecule FRET or quantum efficiencies were determined from donor and acceptor fluorescence intensities after background subtraction and correction for spectral crosstalk and direct acceptor excitation. The apparent FRET efficiency was calculated as,

$$E = \frac{I_A}{I_A + \gamma I_D}$$

where $I_A$and $I_D$are the corrected acceptor and donor intensities, respectively. The γ-factor accounts for correction factor, $\frac{\phi_A X \eta_A}{\phi_D X \eta_D}$ for differences in donor and acceptor quantum efficiencies and detection efficiencies and was determined from donor-only and acceptor-only labeled calmodulin samples measured under identical conditions. Relative quantum efficiencies were estimated by comparing fluorescence intensities of donor and acceptor fluorophores, optical transmission, and detector response. Briefly, relative donor and acceptor quantum efficiencies were incorporated through the experimentally determined γ-factor ~1, which corrects for differences in fluorophore quantum yield and detection efficiency. The γ-factor was obtained using donor-only and acceptor-only labeled calmodulin controls measured under identical experimental conditions. This approach follows established single-molecule FRET methodologies, where relative rather than absolute quantum efficiencies are sufficient for accurate quantification of FRET efficiencies and conformational dynamics.

S3: Table showing FRET efficiency for the given Ficoll70 concentration.

E_{FRET} at different concentration / Distinct Reaction condition	E_{FRET} at 1 mM Ficoll 70	E_{FRET} at 1.5 mM Ficoll 70	E_{FRET} at 2 mM Ficoll 70	E_{FRET} at 2.5 mM Ficoll 70	E_{FRET} at 2.75 mM Ficoll 70	E_{FRET} at 3 mM Ficoll 70	E_{FRET} at 3.2 mM Ficoll 70	E_{FRET} at 3.5 mM Ficoll 70
When eNOS present (No added $CaCl_2$)	0.32±0.07	0.36±0.07	0.39±0.05	0.45±0.06	0.51±0.08	0.51±0.05	0.44±0.07	0.29±0.08
When eNOS absent (No added $CaCl_2$)	0.32±0.06	0.35±0.08	0.40±0.07	0.44±0.07	0.41±0.09	0.42±0.06	0.28±0.07	0.27±0.09

S4: Table presenting the measured FRET efficiencies in the presence and absence of $CaCl_2$.

Different Reaction condition (No added Ficoll 70), $CaCl_2$: 200 μM	FRET Efficiency
Calmodulin + eNOS +$CaCl_2$	0.50±0.068
Calmodulin + eNOS + no $CaCl_2$	0.33±0.069
Calmodulin + no eNOS + $CaCl_2$	0.26±0.064

References:

(1) Westermeier, R.; Scheibe, B. Gel electrophoresis. *A Guide to Theory and Practice* **1993**, *433*, 210-212.
(2) Wang, Z.; Lu, H. P. Single-molecule spectroscopy study of crowding-induced protein spontaneous denature and crowding-perturbed unfolding–folding conformational fluctuation dynamics. *The Journal of Physical Chemistry B* **2018**, *122* (26), 6724-6732.